

# Positive and negative streamers in ambient air: measuring diameter, velocity and dissipated energy

T M P Briels<sup>1</sup>, J Kos<sup>1</sup>, G J J Winands<sup>2</sup>, E M van Veldhuizen<sup>1</sup>  
and U Ebert<sup>1,3</sup>

<sup>1</sup> Department of Applied Physics and <sup>2</sup> Department of Electrical Engineering,  
Technische Universiteit Eindhoven, P O Box 513, 5600 MB Eindhoven, The  
Netherlands,

<sup>3</sup> Centrum voor Wiskunde en Informatica (CWI), P O Box 94079, 1090 GB  
Amsterdam, The Netherlands

E-mail: e.m.v.veldhuizen@tue.nl, ebert@cwi.nl

**Abstract.** Positive and negative streamers are studied in ambient air at 1 bar; they emerge from a needle electrode placed 40 mm above a planar electrode. The amplitudes of the applied voltage pulses range from 5 to 96 kV; most pulses have rise times of 30 ns or shorter. Diameters, velocities and energies of the streamers are measured. Two regimes are identified; a low voltage regime where only positive streamers appear and a high voltage regime where both positive and negative streamers exist. Below 5 kV, no streamers emerge. In the range from 5 to 40 kV, positive streamers form, while the negative discharges only form a glowing cloud at the electrode tip, but no streamers. For 5 to 20 kV, diameters and velocities of the positive streamers have the minimal values of  $d = 0.2$  mm and  $v \approx 10^5$  m/s. For 20 to 40 kV, their diameters increase by a factor 6 while the voltage increases only by a factor 2. Above the transition value of 40 kV, streamers of both polarities form; they strongly resemble each other, though the positive ones propagate further; their diameters continue to increase with applied voltage. For 96 kV, positive streamers attain diameters of 3 mm and velocities of  $4 \cdot 10^6$  m/s, negative streamers are about 20% slower and thinner. An empirical fit formula for the relation between velocity  $v$  and diameter  $d$  is  $v = 0.5 d^2 / (\text{mm ns})$  for both polarities. Streamers of both polarities dissipate energies of the order of several mJ per streamer while crossing the gap.

PACS numbers: 52.80.-s, 52.80.Hc

Submitted to: *The paper is accepted for publication in the cluster issue on “Streamers, Sprites and Lightning” in J. Phys. D: Appl. Phys.*

## 1. Introduction

Streamers of both polarities appear in many phenomena in nature [1, 2, 3]. Industrial applications, on the other hand, have largely focussed on positive (cathode directed) streamers [4, 5, 6, 7, 8, 9, 10, 11, 12, 13, 14, 15, 16, 17, 18, 19, 20, 21] as they are easier to create around sharp tips than negative (anode directed) ones [1]. This even has led to a tendency in the applied physics and electrical engineering literature to use the term "streamer" as equivalent to "positive streamer". Positive streamer coronas are used in gas cleaning and ozone production since they were long thought to have a higher energy efficiency than negative streamer coronas [22]. However, recent investigations with a new generation of pulsed power supplies have shown that negative streamers at voltages of 50 to 80 kV can convert pulsed electric energy into ozone with an unequalled efficiency of 100 g/kWh in ambient air [23, 24]. Furthermore, negative DC-corona is used in dust precipitators to charge small particles that then can be drawn out of a gas stream by an electric field. The properties of these negative streamers at voltages above 50 kV largely resemble those of positive ones [23, 24, 25, 26, 27, 28]. A qualitative similarity between positive and negative streamers in nitrogen with varying oxygen concentration is also found in experiments in a 13 cm gap in protrusion-plane electrode geometry at voltages of 82 to 125 kV [29] while other authors emphasize their difference [30].

Up to now, studies have explored limited parameter regimes, seeing either positive streamers only, or both positive and negative streamers. Here we present a systematic study over a wide parameter regime where actually two regimes are seen, one with positive streamers only and another one with positive and negative streamers. We investigate streamers in ambient laboratory air between a needle and a planar electrode at a distance of 4 cm. We investigate a voltage range from 5 to 96 kV with three different voltage-supplies that were previously used either in the studies of positive streamers at the physics department [31, 32, 33, 34, 35, 36], or for both positive and negative streamers at the electrical engineering department [23, 24, 25, 26, 27, 28] of Eindhoven University of Technology. We attribute similarity or major differences between positive and negative streamers to different voltage ranges. For low voltages, thin positive streamers ignite and propagate easily, while negative discharges require much higher ignition voltages, they form thick and short streamers if at all. For voltages above 60 kV, positive and negative streamers become more and more alike.

Theoretical investigations of the difference between positive and negative streamers in three spatial dimensions (using the cylindrical symmetry of a streamer to calculate effectively in the two dimensions  $r$  and  $z$ ) and including the photo-ionization effect in air are quite rare [37, 38, 39, 40], a thorough discussion and new results that closely correspond to the experimental results of the present paper are presented in [41].

For readers from the geophysical community, a short reminder is in place why we discuss the dependence on applied voltage rather than on applied field. To create streamers efficiently, and to photograph them with high spatial and temporal resolution, streamers in experiments and applications are typically emitted from needle

or wire electrodes that create strong electric fields in their neighborhood.‡ As a short consideration — e.g., of the example for a charged sphere — shows, the electric field close to the strongly curved electrode is mostly determined by voltage and electrode geometry and rather independent of the distance to some distant grounded electrode. It is therefore physically evident and has been confirmed by experiments [31, 32], that streamer inception and initial propagation is determined by applied voltage and electrode geometry, and not by some hypothetical average field within the complete discharge gap. The streamers start in a high field region and consecutively expand into a region with decreasing field.

All streamers presented in this paper are created in a 40 mm gap in a needle to plane electrode geometry in ambient air at atmospheric pressure. We have chosen to investigate the streamers in this gap length because in longer gaps the streamers can branch and form thinner ones [32], and at high voltages in wire-plane electrode geometries they also have been seen to become thicker while propagating [28]; in smaller gaps the streamers have not enough space to develop completely [33, 35], and it is difficult to measure their velocities.

In [35] we concentrated on the investigation of the thinnest positive streamers at varying pressure and gas composition and used voltage supplies with “slow” rise times. In contrast, we here use three voltage supplies with fast rise time to create the thickest streamers possible at the particular peak voltage. The three supplies together cover the voltage range from 5 to 96 kV, their ranges overlap and we find the resulting streamer properties to depend continuously on the voltage, independently of the used supply. We also perform control experiments with one slower voltage supply to further confirm the statement in [32] that power supplies will create similar streamer patterns only if their voltage rise time, peak voltage and internal resistance are similar.

The paper is organized as follows. The experimental setups are described in section 2. The evaluation procedure of photographs and the results are described in section 3; the section is ordered into a general overview, dependence on the voltage supply, stability field, streamer diameters, streamer velocities, an empirical relation between diameter and velocity, and current and energy. Section 4 contains summary and conclusions.

## 2. Experimental setup

### 2.1. Voltage pulse generation

A pulsed power supply consists of three parts: (i) charge storage, (ii) switch, and (iii) load. (i) The charge is conventionally stored in a capacitor, these are readily available for voltages up to 100 kV. (ii) The switch is the crucial part when rise times in the nanosecond range are required. The prevailing choice still is the spark gap, modern

‡ We remark that similar mechanisms can take place next to charged droplets or ice particles in thunderclouds.

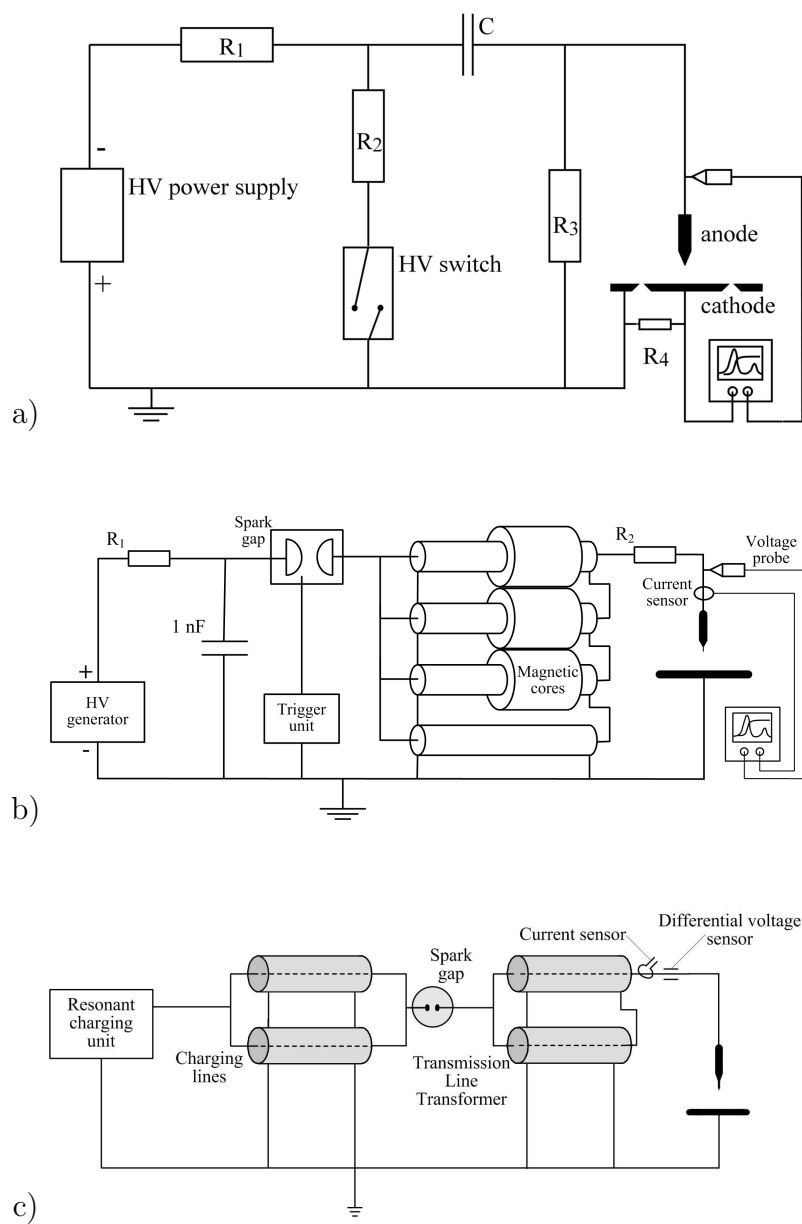


**Figure 1.** a) *C*-supply, b) *TLT*-supply and c) *PM*-supply. *C*-supply and *TLT*-supply were used in the experiments at the physics department and already described in [32]; a detailed drawing of the discharge chamber in these supplies including the current and voltage measurements is provided in Fig. 2 of [35]. The *PM*-supply was used in the experiments at the electrical engineering department and already discussed in [45]; the panel indicates the location of current and voltage measurements. Different diagnostics was used at the two locations as described in the text.

name	$R_1$ (k $\Omega$ )	$R_2$ (M $\Omega$ )	$R_3$ ( $\Omega$ )	$C$ (nF)	$T_{\text{rise}}$ (ns)	$T_{\text{duration}}$ ( $\mu$ s)	range of $U$ (kV)	polarity
C <sub>1</sub>	0	0.004	2.75	0.250	30	1	1 – 60	+
C <sub>2</sub>	2	1	2.75	1	150	1000	1 – 60	+ and –
TLT	1	—	—	1	25	0.05	30 – 60	+
PM	—	—	—	2 (PFL)	15	0.1	40 – 96	+ and –

**Table 1.** Characterization of the electric power supplies in the present experiments. The resistor  $R_1$  influences the rise time of the pulse. The combination of  $R_2$  and  $C$  determines the decay time of the voltage pulse.  $R_3$  is a series resistance to determine the discharge current.

versions combine robustness, high efficiency and long life time [42, 43]. Alternatives such as semiconductors, whether or not in combination with magnetic compression, offer in principle longer life time, but are vulnerable, have lower efficiency and are very expensive. (iii) The load is basically the corona discharge, but impedance matching is a major issue for large systems [44]. The three supplies used in the current study are sketched in Fig. 1; their properties are listed in table 1. In general, the voltage pulse duration is kept short since long pulses at high voltages may allow the initial streamer to develop into a much brighter arc or spark discharge which forms a risk for overexposure of the intensifier of the CCD camera.

The simplest supply is called the C-supply; it was thoroughly described in [32] and it is sketched in Fig. 1(a). In a C-supply, a capacitor first is charged and subsequently discharged over the needle plate gap when the spark gap is closed. It gives the pulse exponential rise and decay times that can be adapted with resistors  $R_1$  and  $R_2$ . Therefore this supply is very versatile and easy to build. Two versions of the C-supply were used as listed in table 1. The C<sub>1</sub>-supply has the advantage of a short rise time  $T_{\text{rise}} = 30$  ns and quite short duration  $T_{\text{duration}} = 1$   $\mu$ s, but this limits the pulse amplitude. The C<sub>2</sub>-supply has a longer rise time  $T_{\text{rise}} = 150$  ns and a longer pulse duration  $T_{\text{duration}} = 1$  ms. It is used to confirm that the streamer structure changes when the rise time becomes too long [32]; the long pulse duration might allow the transition to arc or spark. The C-supplies deliver up to 60 kV.

The pulse amplitude can be increased through a transmission line transformer (TLT) as shown in Fig. 1(b). In a TLT several coaxial cables are connected in series or in parallel at the input or the output side in such a way that either voltage or current is multiplied. A TLT can also be used as impedance matching network between the power source and the corona discharge reactor [44]. The second advantage is that the pulse width and the decay time are very short. This system is further referred to as TLT-supply, it was thoroughly described in [32] as well. Its main characteristics are also listed in table 1; the voltage rise time is 25 ns, and the pulse duration is 50 ns. The voltage range is 30 to 60 kV.

The third supply charges and discharges using coaxial cables. This supply is called

the Power Modulator (PM) supply and will be abbreviated as PM-supply, it is shown in Fig. 1(c). Its output pulses have the same characteristics as the TLT-supply. For charging it uses a pulse forming line (PFL) which leads to a very high wall-plug efficiency (95%). The supply is discussed in more detail in [23, 45]. The rise time of the PM-supply is shorter than that of the TLT-supply, namely 15 ns, probably due to the lower inductance of the load; the pulse duration is 100 ns. This supply has a range from 40 to 96 kV.

## 2.2. Electrical measurements

With the C-supplies, the voltage is measured by a resistive-capacitive divider (Tektronix P6015 for  $C_1$  or Northstar PVM4 for  $C_2$ ) at the positions indicated in Fig. 2 of [35]. The current through the gap is measured with a Pearson current monitor (6585) for  $C_1$  or via the voltage across a small series resistor  $R_s = 2.75\Omega$  between cathode and ground for  $C_2$ . The outer ring across the cathode ensures a well defined, low stray capacity and therefore a fast rise time of the current measurement [46].

With the TLT-supply the voltage and current are measured with the Tektronix high voltage probe (P6015) and a Pearson current monitor (6585), respectively, at the locations indicated in Fig. 1(b). For all three supplies the signals are digitized on an oscilloscope using 0.2 ns sampling time (LeCroy Waverunner 6100A).

The PM-supply at the electrical engineering department uses a differentiating-integrating system to measure the fast high amplitude voltage and current waveforms [47]. In this case a LeCroy Waverunner 2 is used which has the same sampling time. The locations of the measurements are indicated in Fig. 1(c).

## 2.3. Corona enclosure and electrodes

Most measurements – actually those with the C-supplies and the TLT-supply at the physics department – were carried out with the electrodes mounted in a large stainless steel vessel as drawn in Fig. 2 of [35]. This vessel can be evacuated and filled with different gases with pressures in the range of 0.013 to 1 bar, as thoroughly described in [35]. In the present paper, only measurements at standard temperature and pressure in ambient air are presented, and a large window is taken off the sidewall to ensure the refreshment of the air in the vessel. With the PM-supply at the electrical engineering department, that generates voltages up to 96 kV, the streamers propagate in the open air without surrounding vacuum vessel. No significant differences were observed between streamers in open air and in the stainless steel vessel when similar voltage pulses were applied.

All measurements presented in this paper are performed in a 40 mm gap with point-to-plane electrode geometry. We have selected this gap length because in longer gaps, the streamers typically branch and consecutively form thinner and slower streamers [32], while in a 40 mm gap, their diameter and velocity is rather constant. In shorter gaps the streamers don't have enough space to develop fully.

The electrodes are as follows. The needle electrode is made from thoriated tungsten in C<sub>1</sub>- and TLT-supply or from pure tungsten in C<sub>2</sub>- and PM-supply. No differences in streamer pattern are observed between these two needles. The tip is spherical with radius  $\approx 15 \mu\text{m}$ , a cone of height 2 mm connects the tip to a cylinder with radius 0.5 mm; these shapes are not perfect, the surface has microscopic scratches from the grinding process; even a dropped and misformed asymmetric needle does not create visibly different discharge structures. Furthermore, for the C-supplies and the TLT-supply, the plate electrode is made from stainless steel, while for the PM-supply, it is from aluminum.

#### 2.4. CCD-cameras and image data evaluation

At the physics department, the discharges generated with the C-supplies and the TLT-supply are photographed with a 4QuikE intensified CCD camera from Stanford Computer Optics as described in [35]. The camera has  $1360 \times 1024$  pixels and a minimal exposure time of 2 ns. In the wave length range of 200 - 800 nm, it has a quantum efficiency of  $\approx 0.3$  on average. Each pixel has 12 bit, and different gains can be chosen. The discharges generated with the PM-supply in the electrical engineering department are photographed with a Princeton Instruments 576G/RB intensified CCD-camera as described in [45]. It should be noted that if the initial streamer channels later evolve into arcs, the intensifier of the cameras could be damaged even after exposure. Therefore a transition into an arc is carefully avoided by keeping the voltage pulse sufficiently short.

A number of pictures are shown in our articles. However, it must be noted that the actual pictures depend on the chosen representation of the raw data; this is demonstrated in panels a and b of Fig. A2 of [35]. An example of the actual data together with a picture is shown in Fig. 5 of [32]; profile bars of the real data along two sections through the image are shown on the margin. Streamer diameters are evaluated as the full width at half maximum (FWHM) from this original data. The further evaluation procedure is described in section 3.4.

### 3. Measurements and results

#### 3.1. Streamer structures as function of voltage and polarity — an overview

As a first overview, Figure 2 shows representative pictures of the discharges as a function of voltage and polarity. The panels show the complete streamer evolution in a 40 mm point-plane gap in air at 1 bar, i.e., with a sufficiently long exposure time of the photograph. In panels a and b, the slow C<sub>2</sub>-supply with the long pulse duration is used together with the equipment at the physics department. No secondary streamers or return strokes appear after the primary streamers at voltages as low as 20 kV, and the panels just show the primary discharge. In panels c to f, the PM-supply with a voltage pulse duration of 100 ns is used together with the equipment at the electrical engineering department; the images show the streamers during the complete

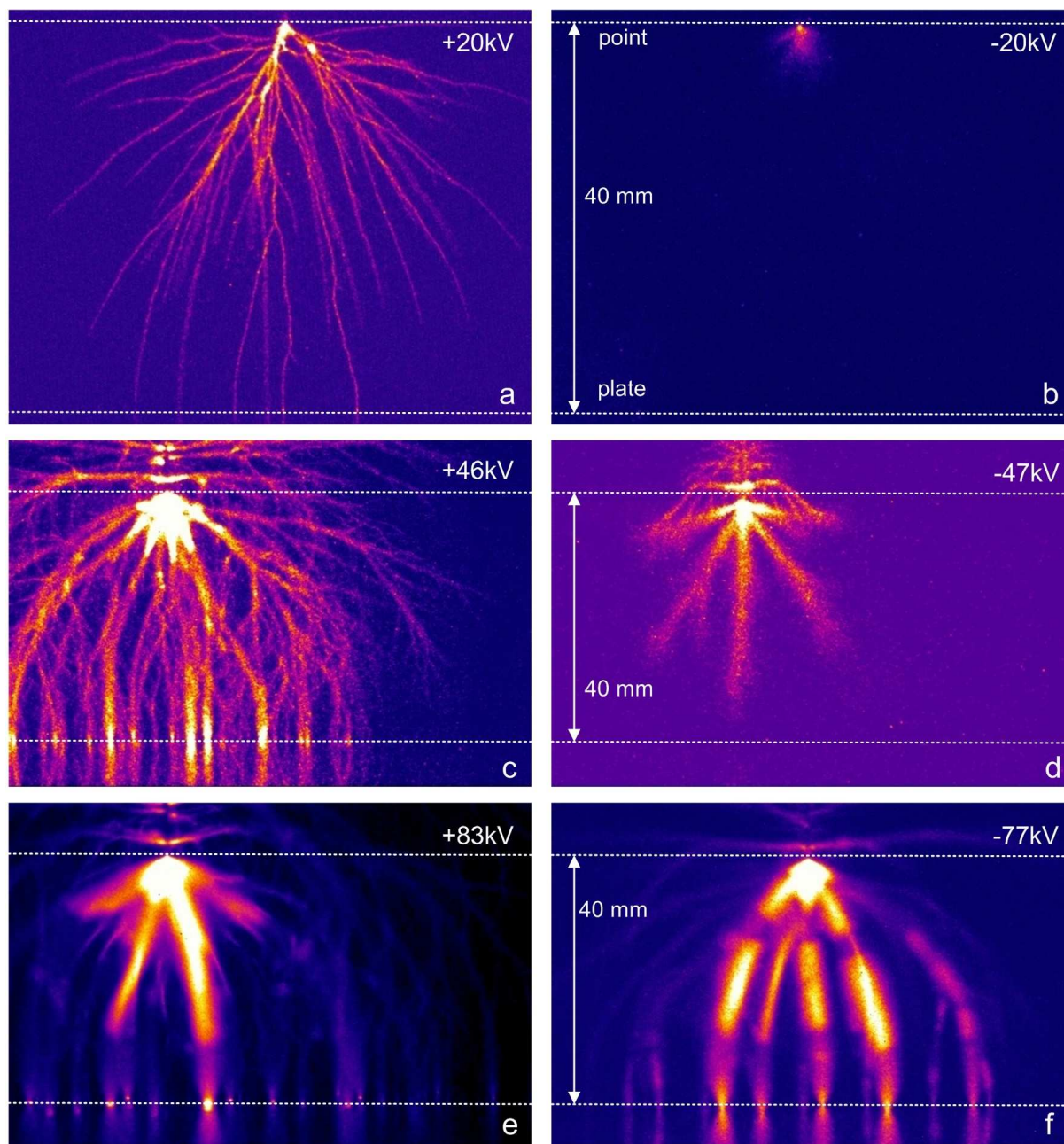


**Figure 2.** Time integrated photographs of positive (left column) and negative (right column) streamers in a 40 mm gap in air at 1 bar. The applied voltages are indicated in the upper right corner of each panel, they are  $\approx \pm 20$  kV in the upper row,  $\approx \pm 46$  kV in the middle row, and  $\approx \pm 80$  kV in the lower row. The discharges in panels a and b were made with the  $C_2$ -supply at the physics department, and those in panels c - f with the PM-supply at the electrical engineering department; therefore different cameras etc. were used. The white dotted lines indicate the position of the plate electrode below and the height of the needle electrode tip above.

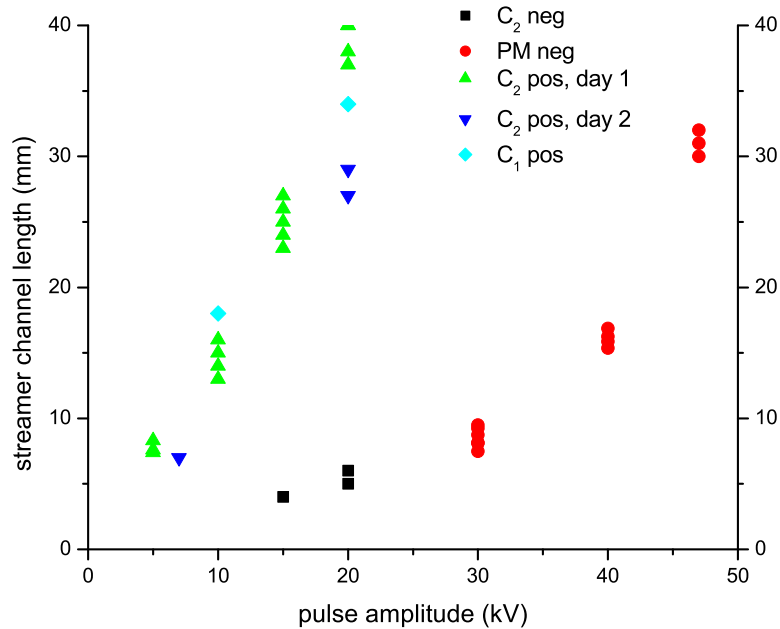


**Figure 3.** Maximal streamer channel length as a function of voltage and polarity. The lengths are limited by the distance between electrodes which is 40 mm. The longest streamers in each image are evaluated, they typically move straight downward. Power supplies  $C_1$ ,  $C_2$  or PM are used as indicated in the figure. For positive streamers created by the  $C_2$ -supply, the data for two different measurement days are shown, they indicate a typical variation between days. Discharges below an extension of 10 mm are mostly cloud shaped and will not be called streamers.

pulse duration. Streamers similar to those in panels c and d have also been generated with the  $C_1$ - or the  $C_2$ -supply in the physics department; in particular, the temporal evolution of positive discharges similar to panel c are described in detail in [32]. The initial evolution of negative streamers similar to panel d is shown in Fig. 4 below. The white dotted lines indicate the approximate position of the plate electrode below and the height of the needle electrode tip above. It can be seen that at high voltages, streamers are emitted from the complete needle electrode, not only from its tip. Below the electrode spots in panels c, e and f, mirror images can be seen; they are reflected from the planar electrode. The white lines do not precisely intersect with the foot points of all streamers as the camera slightly looks down onto the electrode and the discharge is a three-dimensional structure. This 3D structure can be resolved with stereographic imaging, for first results, we refer to [36].

Figure 3 complements figure 2, it shows the maximal length of the streamer channels as a function of voltage and polarity. The figures illustrate our statement that there are two regimes with a smooth transition zone, a regime of voltages below 40 kV where positive and negative discharges can be clearly distinguished, and a regime above 60 kV where they are quite similar. This will now be elaborated in more detail.

Below 40 kV, positive and negative discharges are remarkably different. Positive discharges ignite above 5 kV, while negative discharges are only seen above 15 kV. When the voltage on the positive discharges increases from 5 to 20 kV, thin streamers of increasing lengths form that branch frequently (for a further characterization of branching, we refer to [32, 35, 36]); their lengths as a function of voltage are shown in figure 3. They bridge the gap above 20 kV as shown in figure 2a. At this same voltage, the negative discharge only forms a small cloud around the tip and no streamer, as can be seen in figure 2b§. Negative streamers form above 30 kV, but they are then still too short to determine their diameters. Whenever their diameter can be determined, they are much thicker than the 0.2 mm diameter observed for the thinnest positive streamers. Negative streamers bridge the complete 40 mm gap only at voltages above 50 kV as shown in figure 3. Panels c and d in figure 2 show positive and negative streamers at 46 kV where both are 1 to 2 mm thick but the negative ones do not reach the plate electrode and hardly branch while the positive streamers cross the gap and form many branches. In both cases, the discharge emerges not only from the needle tip, but also above it, most likely at sharp edges.

Above 60 kV, positive and negative streamers become increasingly more alike. The negative streamers cross the electrode gap at 56 kV (figure 4). At voltages above 75 kV, streamers of both polarities are 2 to 3 mm thick, bridge the gap and hardly branch. The positive streamers still branch a little more than the negative ones (see panels e and f in figure 2).

We remark that figure 2f shows an overexposed streamer region in the middle of the gap while the regions near the tip and near the plate are darker. The length of this region increases with increasing voltage from 16 mm through 18 mm to 23 mm at 64 kV, 75 kV and 82 kV, respectively. It arises *after* the primary streamers have bridged the electrode gap (where "primary streamer" denotes the first group of streamers after the voltage has been applied [48]). It is not known why this large region forms in the middle of the gap; usually such a region stretches out from the tip and is interpreted as a secondary streamer or as a glow developing along the trails of the primary streamers (as in figure 2e). Striated or subdivided secondary streamers are also reported in [48], however, without photographs. The spots on the plate electrodes also appear after the streamer has crossed the gap; the cathode spots appear more or less spherical, whereas anode spots are contracted at the plate but become broader and diffuser above the surface; they continue into the streamer more gradually.

### 3.2. Dependence on the voltage supply

It should be noted that the streamers in figure 2 are created with the C<sub>2</sub>-supply at 20 kV and with the PM-supply at higher voltages. For positive streamers at voltages of at least 30 kV, we have shown in [32] that the slow voltage rise time of the C<sub>2</sub>-supply

§ The positive streamers also start from a cloud [33, 35] although this cloud is not always visible, especially at atmospheric pressure.

creates thinner channels than the other supplies as the streamers start to propagate before the voltage has reached its maximal value; this observation is also confirmed in the present measurements as demonstrated in panels b and c in figure 6; these panels show positive streamer discharges at the same peak voltage of  $\approx 40$  kV, but for voltage rise times of 30 or 150 ns, respectively. However, at 20 kV positive streamers do not show this supply dependence as the streamer inception seems to be sufficiently slow at such low voltages.

One might wonder whether a similar supply dependence holds for negative streamers, but we have no evidence for it. Furthermore, one can speculate whether the negative streamers in figure 2(d) do not cross the gap because the voltage pulse duration in the PM-supply is only 100 ns; if the streamer inception time would be several tens of nanoseconds, the remaining pulse duration could be insufficient to let the streamers cross the gap. To test these hypotheses, we have plotted the measured lengths of negative streamers as a function voltage in figure 3. The streamers at 15 and 20 kV are created with the C<sub>2</sub>-supply, and for voltages of 30 kV and larger with the PM-supply. The figure shows that the data follow a smooth curve across the change of supplies; this suggests that the negative streamers are more robust against changes of the power supplies than the positive ones, and that the negative streamers in figure 2 have reached their maximal length during the 100 ns duration of the voltage pulse of the PM-supply.

### 3.3. Stability field

A common hypothesis is that there is a stability field, i.e., a minimal field that the streamer needs to propagate; this field would also be the characteristic field inside the streamer [1, 49]. This hypothesis is guided by the empirical observation, that the ratio of applied voltage over maximal streamer length is approximately constant for a given gas and polarity; this ratio has the dimension of an electric field. (The role of some hypothetical average background field is discussed in the introduction.) For positive streamers in point-plane and plane-plane gaps in air, a value of 4.4 to 5 kV/cm is fitted to experiments in [1, 49] and references therein. The data for positive streamers in figure 3 is fitted by  $U/L = 6 \pm 1$  kV/cm, which is in agreement with the above values within the error bar. For negative streamers, typical field values in the literature are a factor 2 or 3 higher [1, 37]. Such values can also be fitted to our data for negative streamer in figure 3; however, it should be noted that the length is certainly not a linear function of the voltage in this curve, also because there are no negative streamers below 40 kV, and that the approximation of a constant stability field for negative streamers is questionable in view of this data.

### 3.4. Streamer head diameters

The streamer head diameters are determined from iCCD-images such as in figure 4d; for the evaluation of the raw data imaged in such figures, we refer to section 2.4. The full

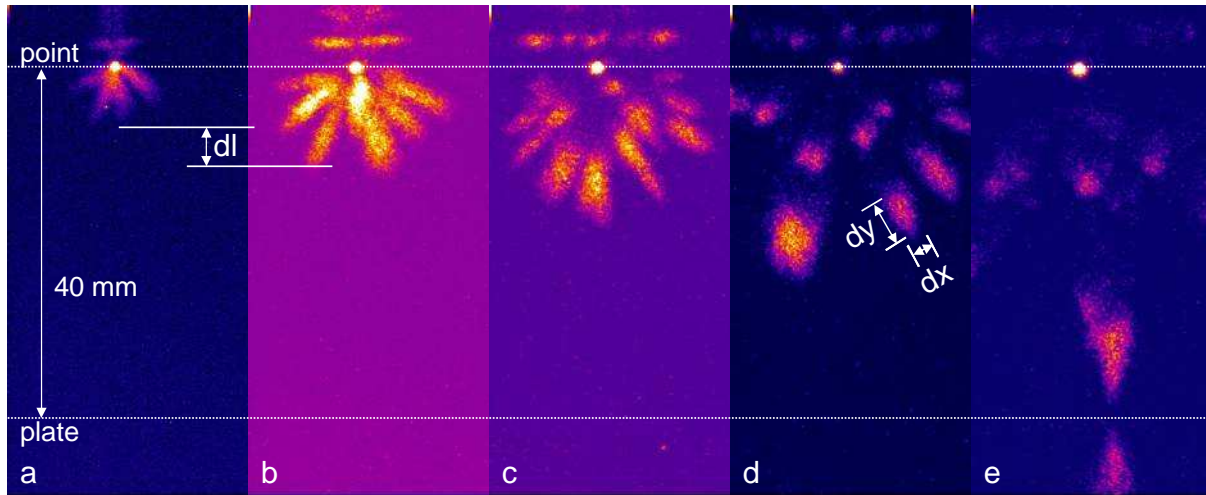


**Figure 4.** Negative streamers at -56 kV generated with the PM-supply. The exposure time of each picture is about 5 ns. The gate delay is (a) 4.4 ns, (b) 9.3 ns, (c) 14.3 ns, (d) 19.6 ns, (e) 28.8 ns. The white lines indicate the position of the electrodes as in Fig. 2. The light at the bottom of figure (e) is a reflection of the streamer light on the anode plate. How velocities are determined from such data, is described in Section 3.5.

width  $dx$  at half maximum (FWHM) is measured and averaged over the  $dy$ -direction for as long as the streamer channel is straight to suppress the stochastic single photon fluctuations within the pixels of the camera. The same definition of the diameter was also used in [32, 33, 35]. Only single in-focus streamers at a place without return stroke or electrode effects are evaluated, typically in the middle of the electrode gap. Depending on voltage and polarity, typically three to ten streamers per photograph were evaluated, and the diameters were furthermore averaged over three to five photographs per voltage. In the measurements with the PM-supply, secondary streamers can appear after the primary streamers have crossed the gap, and occasionally secondary streamers are evaluated instead of primary streamers when there are not sufficiently many suitable primary streamer channels. However, primary or secondary streamer diameter show no significant difference with the PM-supply with its high voltages, as also reported in [27, 28].

The diameters of positive and negative streamers as a function of applied voltage are shown in figure 5. The different power supplies and polarities are indicated with symbols. The measurements of positive streamers with supplies  $C_1$ , TLT and PM together span a continuous curve within the error bars, consistently with what we found in [32]. The positive streamers created with the  $C_2$ -supply remain thin when the peak voltage increases, as is illustrated in panel b of figure 6; this is also consistent with [32]. In this case, the streamers already start to propagate while the voltage is still below its saturation value; furthermore their current is limited by the large series resistance  $R_3$ . For negative streamers, diameters are only measured for experiments performed with the PM-supply.

Positive streamers ignite above 5 kV. As shown in figure 5, their diameter then is

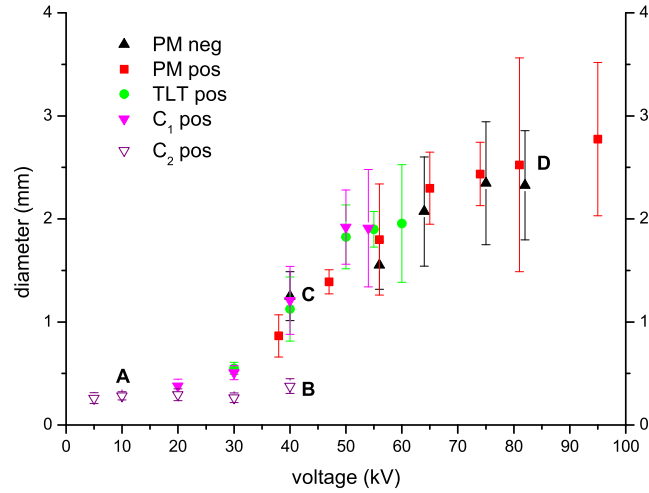


**Figure 5.** Diameters of positive and negative streamers as a function of applied voltage. The symbols indicate the different voltage supplies and polarities. The letters A, B, C, and D indicate where photographs of positive streamers are included; they are shown in panels a, b, and c of figure 6 for A, B and C, and in figure 2e for D.

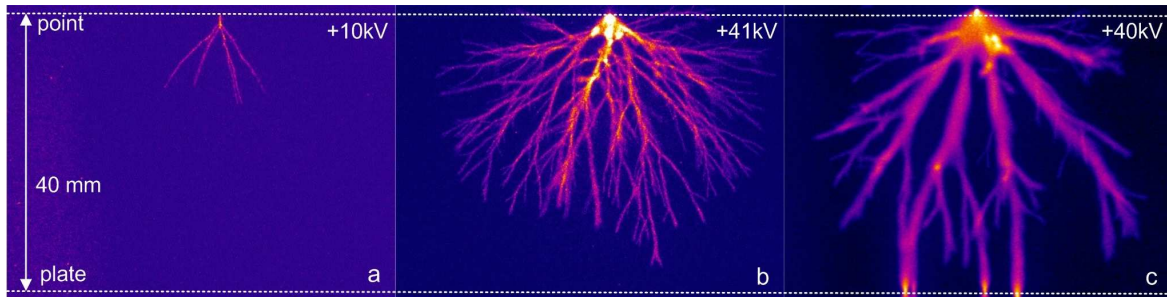


**Figure 6.** Typical photographs of positive streamers for parameter values indicated by A, B, C in figure 5. Panels a and b are made with the slow C<sub>2</sub>-supply, panel c with the fast C<sub>1</sub>-supply. The maximal voltage is a) +10 kV, b) +41 kV, and c) +40 kV. The white dotted lines indicate the electrode positions as in Figs. 2 and 4. The streamers in panel a at 10 kV have reached their maximal length; the streamers in panels b and c at  $\approx 40$  kV are still propagating. Panels b and c demonstrate how strongly positive streamers at a voltage saturation value of 40 kV depend on the voltage rise time of the supply, as discussed in [32].

0.2 mm, i.e., the minimal diameter [32, 35]. For 20 kV, their diameter is 0.4 mm, and the streamers bridge the 40 mm gap for the first time. Then the diameter increases by a factor of 10 (i.e., from 0.2 to 2 mm) when the applied voltage increases only by a factor of  $\approx 2$  (from 25 to 55 kV). Above 55 kV, the diameter continues to increase, but less rapidly; it reaches 3 mm at 96 kV. Whether for higher voltages, the diameter can become even higher, or whether it saturates eventually, is an open question. We observed that at very high voltages, e.g. at +82 kV in figure 8a, the voltage rise time of the PM-supply again becomes comparable to the streamer inception time as the

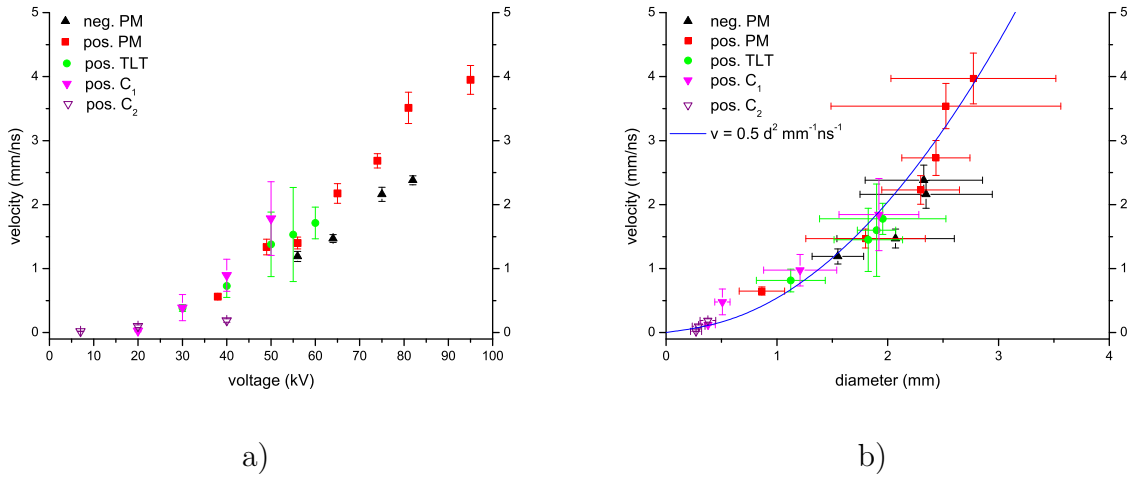


**Figure 7.** a) Velocity of positive and negative streamers in air at standard temperature and pressure as a function of voltage in a 4 cm gap. b) Velocity plotted as function of diameter. The line indicates a fit with  $v = 0.5 d^2 / (\text{mm ns})$ .

inception time decreases with increasing voltage; this entails that at high voltages the streamers start before the voltage has saturated. This is also observed in [28] with the same PM-supply at +74 kV, while it is not observed at -72 kV, in agreement with the discussion in Section 3.2.

The negative discharge becomes visible at 15 kV, but does not yet form streamers. The diameter of the negative streamers can be measured at voltages of 40 kV or higher. For 40 kV the diameter is 1.2 mm. The negative streamers bridge the gap for the first time at  $\approx 56$  kV (figure 4) with a diameter of 1.5 mm. Their diameter increases with applied voltage to  $\approx 2.3$  mm for voltages between 76 and 82 kV. On average, the positive streamers are about 10% thicker than the negative ones, but this difference is within the error margins.

### 3.5. Streamer velocities

In the experiments at the physics department with the C-supplies and the TLT-supply, the light trace on the photographs can be interpreted as the path that the streamer head has followed during the exposure time of the camera [50]; therefore the streamer velocities are measured as the full width at half maximum (FWHM) of the length  $dy$  in the propagation direction, divided by the exposure time  $\Delta t$  of the camera; the procedure is illustrated in figure 4. To minimize the error, sufficiently long exposure times are used such that the streamer head crosses 1/4th to 1/8th of the electrode gap; these times are 10 to 100 ns; the method is further described in [35]. The velocities are evaluated at some distance from the electrodes; typically three to ten streamers per photograph and three to five photographs per voltage are evaluated. In the presently investigated 40 mm gap, the streamer velocity and diameter are approximately constant. In contrast, in the case of a 160 mm electrode gap the streamer velocity does depend on the position

and diminishes after branching [35].

In the experiments at the electrical engineering department with the PM-supply, the velocities are measured as the propagation distance between photographs ( $dl$  in figure 4a,b) divided by the difference in delay time  $T$  of the photographs, where each photograph is taken during a different discharge pulse. The streamers that have propagated furthest are evaluated in each picture, they predominantly move straight downward. This method can be used since the jitter in streamer inception at high voltages is as small as about 1 ns [23, 27]. Five to ten photographs with different delays (e.g., the five pictures in figure 4) are taken per voltage, depending on the gap transit time of the streamer. Position is plotted as a function of time for each photograph and an average velocity is determined graphically. One or two propagation sequences per voltage are evaluated. Only the fastest streamers are used since they propagate most parallel to the camera's focal plane. Again the velocity is found to be constant throughout the gap [23, 27].

We remark that the ambiguity of the two-dimensional images of the three-dimensional discharge can lead to an underestimation of the velocities that is counteracted by evaluating only the fastest streamers. Velocity measurements with the stereographic imaging method introduced in [36] are currently under way.

Figure 7a shows the resulting velocities of positive and negative streamers as a function of voltage. The velocities of streamers of both polarities increase almost linearly with voltage. Velocities of negative streamers at voltages lower than 56 kV could not be measured because the streamers did not propagate far enough to measure them reliably. Note that the velocity of positive streamers increases rapidly in this range, from 0.2 mm/ns at 20 kV to  $\approx 1.5$  mm/ns at 56 kV. Figure 7a shows that the negative streamers are about 25% slower than the positive ones when their velocities can be measured.

### 3.6. An empirical relation between diameter and velocity

In figure 7b the velocity is plotted as a function of the diameter; the data is extracted from figures 5 and 7a. The figure shows that the velocity  $v$  increases with increasing diameter  $d$ ; it can be fitted quite well by the empirical equation  $v = 0.5 d^2 / (\text{mm ns})$  where  $v$  and  $d$  are measured in their natural units. The approximation also works well for streamers of intermediate radius as measured in [23, 27, 28]. However, streamers with a minimal diameter of about 0.2 mm [32, 35] are a factor 5 too slow in this approximation. The velocities of the thin streamers with diameters less than 0.5 mm in [30, 51, 17] are also underestimated by a factor of about 4.

### 3.7. Current and energy

A typical evolution of current and voltage for positive and negative streamers with the PM-supply is shown in Fig. 8, the generated discharges are shown in panels e and f of Fig. 2. The voltage pulse reaches approximately  $\pm 80$  kV and lasts for about 100 ns. While the voltage  $U$  rises, it creates a capacitive current  $I_{\text{capacitive}} = C_{\text{geom}} dU/dt$  in the

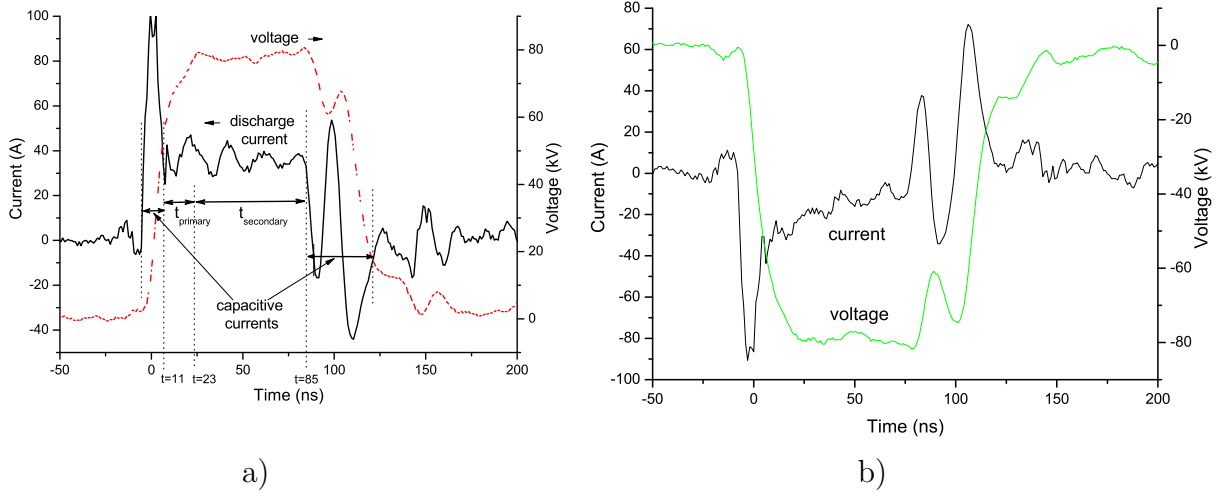


**Figure 8.** Evolution of current and voltage for  $\approx 82$  kV for a) positive and b) negative streamers generated with the PM-supply. The generated discharges are shown in panels e and f of fig. 2. The current and voltage lines are smoothed by averaging over 5 adjacent points. In panel a, characteristic times and capacitive versus discharge currents are indicated, as discussed in the text.

circuit;  $C_{geom}$  is the capacitance of the discharge vessel in the absence of a discharge. The capacitive currents are indicated in panel a of Fig. 8. After approximately 11 ns (as indicated in the figure), the current is mainly the discharge current; its maximum is approximately 45 A for both polarities. The positive discharge current remains at this level for the duration of the voltage pulse (a plateau of duration  $\approx 80$  ns); the oscillations are due to imperfect matching with the external circuit. The negative discharge current does not have this plateau but slowly decreases to 10 A before the voltage pulse drops back to zero.

Estimates for the dissipated energies within the complete discharge are shown in figure 9; they are calculated by integrating the product of voltage and current over time, after the capacitive part of the total current is subtracted [30]. The total energy of the discharge is calculated by integrating to 200 ns when the voltage pulse certainly has finished.

Fig. 4 illustrates that the first group of streamers, the so-called primary streamers [48], cross the gap within 27 ns for  $-56$  kV. This gap crossing time varies from 80 ns for 30 kV to 10 ns for 96 kV for positive streamers, and from 27 ns for 56 kV to 15 ns for 83 kV for negative ones. At a later time, secondary processes occur as described elsewhere, see e.g. [23, 28, 32]. The energy of the primary streamers is calculated by integrating from 11 ns (when the total current becomes larger than the capacitive current, i.e., when the particle current begins to flow) to the time when the primary streamers have bridged the gap. This arrival time is estimated from the streamer velocity according to section 3.5. For 82 kV, it is 12 ns, therefore duration of the primary streamers  $t_{primary}$  is assumed to last from  $t = 11$  ns to  $t = 23$  ns, as

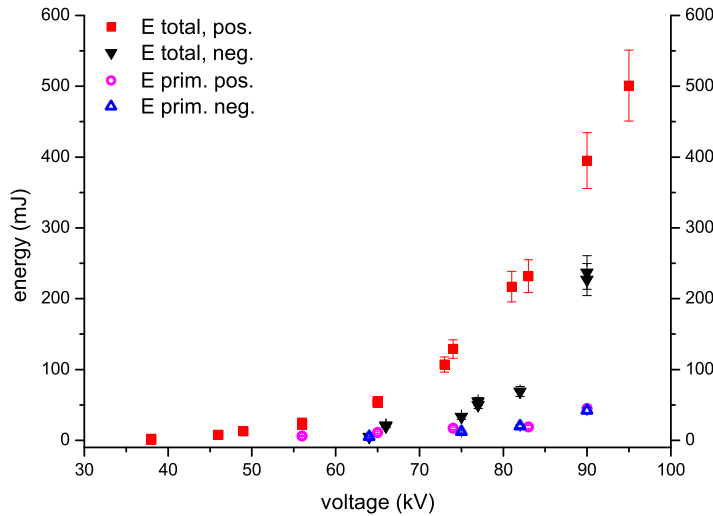


**Figure 9.** Dissipated energy of the total discharge and of the primary positive and negative streamers only as a function of voltage. The PM-supply was used.

indicated in panel a of Fig. 8.

Figure 9 shows that the total energy of positive discharges is higher than for negative discharges. This is because the current persists longer in the positive discharge while it decreases for the negative ones (figure 8). The energy of the primary streamers is also shown in figure 9. Though these values must be regarded as an estimate, the data are similar for positive and negative streamers. These energies are never higher than 50 mJ and thus are considerably lower than the total energy which is maximally 400 mJ for a positive discharge and 220 mJ for a negative one at 90 kV. Our observation that positive and negative streamers have similar energies, is consistent with [23, 27, 28].

#### 4. Summary and conclusions

Our measurements indicate that the inception and propagation processes of positive and negative streamers in ambient air are quite different. Positive streamers emerge when a voltage of at least 5 kV is applied to a needle electrode at 4 cm distance from a planar grounded electrode, while negative streamers only propagate above 40 kV (which is around the DC-breakdown voltage of the gap). Two regimes have to be distinguished.

- 1)  $5 \text{ kV} < U < 40 \text{ kV}$ : Positive streamers propagate. Their diameters increase from 0.2 mm at 5 kV to 1 mm at 40 kV, they bridge the complete electrode gap above 20 kV and they branch. Their velocity ranges from  $10^5 \text{ m/s}$  at 5 kV to  $10^6 \text{ m/s}$  at 40 kV. A negative discharge is only visible above 20 kV as a glowing cloud near the electrode tip; no negative streamers are formed.
- 2)  $U > 40 \text{ kV}$ : Negative streamers appear, but they do not cross the gap for voltage below 56 kV. Positive and negative streamers have a similar diameter of 1 mm at

40 kV that increases up to 3 mm for 96 kV. The positive streamer velocity increases from  $10^6$  m/s at 40 kV to  $4 \cdot 10^6$  m/s at 96 kV. The velocity of negative streamers can only be measured for voltages higher than 56 kV which is then about 25% lower than for positive ones. The energy of the primary positive and negative streamers are similar; it ranges from 20 to 50 mJ for voltages from 74 to 90 kV.

We also find the completely empirical fit  $v = 0.5d^2/(\text{mm ns})$  for the relation between velocity  $v$  and diameter  $d$  of positive and negative streamers.

As a counterpart to the present experimental investigation of streamers of both polarities, a theoretical investigation is presented in [41]. In that paper, the low voltage regime is investigated, and a strong asymmetry between short positive and negative streamers is found, in agreement with the present experiments. In particular, positive simulation streamers next to needle electrodes easily evolve out of some initial ionization seed; they have small diameters comparable to experiments and a strong field enhancement at the streamer tip; this field enhancement allows them to propagate into the regions with lower background fields further away from the needle electrode. In these simulations, we find approximately the same empirical relation between velocity and diameter for short positive streamers as in panel b of Fig. 7. On the other hand, negative simulation streamers evolve as well out of some initial ionization seed in the high field region next to the electrode needle; but then their diameter increases when penetrating the regions with lower fields; therefore the field is less enhanced and they easily extinguish. We conclude that the simulations presented in [41] do allow to understand essential physical features of the low voltage regime of the experiments presented here.

## Acknowledgments

This work is financially supported by STW under contract number 06501 and by NWO under contract number 047.016.017.

## References

- [1] Raizer Yu P 1991, *Gas Discharge Physics*, Berlin: Springer
- [2] Bazelyan E M, Raizer Yu P 1998, *Spark Discharge* (CRC Press, Boca Raton, Florida)
- [3] Williams E R 2006, *Plasma Sources Sci. Technol.* **15** S91
- [4] Wagner K H 1966, *Z. Physik* **189** 465
- [5] Phelps C T, and R F Griffiths 1976, *J. Appl. Phys.* **47**, 2929-2934
- [6] Marode E 1975, *J. Appl. Phys.* **46** 2005-2015
- [7] Bastien F, and E Marode 1979, *J. Phys. D: Appl. Phys.* **12** 249-263
- [8] Spyrou N, and C Manassis 1989, *J. Phys. D: Appl. Phys.* **22** 120-128
- [9] Tajalli H, D W Lamb, and G A Woolsey 1989, *J. Phys. D: Appl. Phys.* **22** 1497-1503
- [10] Creighton Y L M 1994, *Pulsed Positive Corona Discharges: Fundamental Study and Application to Flue Gas Treatment*, PhD thesis, Eindhoven University of Technology, The Netherlands. Available on <http://alexandria.tue.nl/extra3/proefschrift/PRF10A/9402886.pdf>
- [11] Allen N L, and A Ghaffar 1995, *J. Phys. D: Appl. Phys.* **28** 331

- [12] Alexandrov N L, and E M Bazelyan 1996, *J. Phys. D: Appl. Phys.* **29** 2873
- [13] Pancheshnyi S, S Sobakin, S Starikovskaia, and A Starikovskii 2000, *Plasma Physics Reports* **26** 1054-1065
- [14] Pancheshnyi S, S M Starikovskaia, and A Y Starikovskii 2001, *J. Phys. D: Appl. Phys.* **34** 105-115
- [15] Pancheshnyi S and A Starikovskii 2003, *J. Phys. D: Appl. Phys.* **36** 2683-2691
- [16] Pancheshnyi S and A Starikovskii 2004, *Plasma Sources Sci. Technol.* **13** B1-B5
- [17] Pancheshnyi S, M Nudnova, and A Starikovskii 2005, *Phys. Rev. E* **71** 016407
- [18] Pancheshnyi S 2005, *Plasma Sources Sci. Techn.* **14** 645-653
- [19] Ono R, and Oda T 2003, *J. Phys. D: Appl. Phys.* **36** 1952-1958
- [20] Ono R, and Oda T 2005, *J. Phys. D: Appl. Phys.* **37** 730-735
- [21] Ono R, and Oda T 2008, *J. Phys. D: Appl. Phys.* **41** 035204
- [22] van Veldhuizen E M (ed.) 2000, *Electrical Discharges for Environmental Purposes: Fundamentals and Applications*, Huntington: Nova Science Publishers
- [23] Winands G J J 2007, *Efficient streamer plasma generation*, PhD thesis, Eindhoven University of Technology, The Netherlands. Available on <http://alexandria.tue.nl/extra2/200710708.pdf>
- [24] van Heesch E J M, G J J Winands, and A J M Pemen, *Evaluation of pulsed streamer corona experiments to determine the O\* radical yield*, submitted to *J. Phys. D: Appl. Phys.*, cluster issue on "Streamers, Sprites and Lightning"
- [25] Blom P P M, Smit C, Lemmens R H P and van Heesch E J M 1994, *Combined optical and electrical measurements on pulsed corona discharges Gaseous Dielectrics*, vol VII, ed: Christophorou L G and James D R (New York: Plenum)
- [26] Blom P P M 1994, *High-Power Pulsed Corona*, PhD thesis, Eindhoven University of Technology, The Netherlands. Available on <http://alexandria.tue.nl/extra1/PRF14A/9702338.pdf>
- [27] Winands G J J, Liu Z, van Heesch E J M, Pemen A J M and Yan K 2008, *ADS and CDS streamer generation as function of pulse parameters*, *IEEE Trans. Plasma Sci.* [to appear]
- [28] Winands G J J, Liu Z, Pemen A J M, van Heesch E J M, Yan K, *Analysis of streamer properties in air as function of pulse and reactor parameters by ICCD photography*, *J. Phys. D: Appl. Phys.* [accepted for special issue on "Streamers, Sprites and Lightning"]
- [29] Yi W J and Williams P F 2002, *J. Phys. D: Appl. Phys.* **35** 205
- [30] van Veldhuizen E M and Rutgers W R 2002, *J. Phys. D: Appl. Phys.* **35** 2169
- [31] Briels T M P, van Veldhuizen E M and Ebert U 2004, *Experiments on propagating and branching streamers in air*, proceedings XV Int. Conf. on Gas Discharges and Applications <http://gd2004.ups.tlse.fr>, available through <http://homepages.cwi.nl/~ebert/GD2004-Corona.pdf>
- [32] Briels T M P, Kos J, van Veldhuizen E M and Ebert U 2006, *J. Phys. D: Appl. Phys.* **39** 5201
- [33] Briels T M P, van Veldhuizen E M and Ebert U 2008, *Time resolved measurements of streamer inception in air*, *IEEE Trans. Plasma Sci.* [in print]
- [34] Briels T M P, van Veldhuizen E M, Ebert U 2008, *Positive streamers in ambient air and a N<sub>2</sub>:O<sub>2</sub>-mixture (99.8:0.2)*, *IEEE Trans. Plasma Sci.* [in print]
- [35] Briels T M P, van Veldhuizen E M and Ebert U 2008, *Positive streamers in air and nitrogen of varying density: experiments on similarity laws*, cluster issue on "Streamers, Sprites and Lightning" in *J. Phys. D: Appl. Phys.* [to appear] *ArXiv.org e-prints*: 0805.1364
- [36] Nijdam S, Moerman J S, Briels T M P, van Veldhuizen E M, Ebert U 2008, *Appl. Phys. Lett.* **92** 101502
- [37] Babaeva N Y and Naidis G V 1997, *IEEE Trans. Plasma Sci.* **25** 375
- [38] Liu N, Pasko V P 2004, *J. Geophys. Res.* **109** A04301
- [39] Luque A, Ebert U, Montijn C, Hundsdorfer W 2007, *Appl. Phys. Lett.* **90**, 1501
- [40] Luque A, Ebert U, Hundsdorfer W 2007, *ArXiv.org e-prints*: 0712.2774.
- [41] Luque A, Ratushnaya V, Ebert U 2008, *Positive and negative streamers in ambient air: modeling evolution and velocities*, revised for the cluster issue on "Streamers, Sprites and Lightning" in *J. Phys. D: Appl. Phys.*, *ArXiv.org e-prints*: 0804.3539

- [42] Winands G J J, Liu Z, Pemen A J M, van Heesch E J M, and Yan K 2005, *Rev. Sci. Instrum.* **76** 085107
- [43] Liu Z, Yan K, Winands G J J, Pemen A J M, van Heesch E J M, and Pawelek D B 2006, *Rev. Sci. Instrum.* **77** 073501
- [44] Yan K 2001 *Corona plasma generation* PhD Thesis Technische Universiteit Eindhoven, available through <http://alexandria.tue.nl/extra2/200142096.pdf>
- [45] Winands G J J, Liu Z, Pemen A J M, van Heesch E J M, Yan K and van Veldhuizen E M 2006, *J. Phys. D: Appl. Phys.* **39** 3010-3017
- [46] Gravendeel B 1987, *Negative corona discharges: A fundamental study*, PhD thesis, Eindhoven University of Technology, The Netherlands. Available through <http://alexandria.tue.nl/extra3/proefschrift/PRF5A/8612916.pdf>.
- [47] van Houten M A, *Electromagnetic compatibility in high voltage engineering*, Ph.D. thesis, Eindhoven University of Technology, the Netherlands (1990). Available on [www.tue.nl/bib](http://www.tue.nl/bib).
- [48] Sigmund R S 1984, *J. Appl. Phys.* **56** 1355
- [49] Allen N L and Ghaffar A 1995, *J. Phys. D: Appl. Phys.* **28** 331
- [50] Ebert U, Montijn C, Briels T M P, Hundsdorfer W, Meulenbroek B, Rocco A and van Veldhuizen E M 2006, *Plasma Sources Sci. Technol.* **15** S118
- [51] van Veldhuizen E M and Rutgers W R, *J. Phys. D: Appl. Phys.* **36** (2003) 2692.